



Title	Transformation of beneficially reused aluminium sludge to potential P and Al resource after employing as P-trapping material for wastewater treatment in constructed wetland
Authors(s)	Zhao, X.H., Zhao, Y.Q., Kearney, P.
Publication date	2011-10-15
Publication information	Zhao, X.H., Y.Q. Zhao, and P. Kearney. "Transformation of Beneficially Reused Aluminium Sludge to Potential P and Al Resource after Employing as P-Trapping Material for Wastewater Treatment in Constructed Wetland." Elsevier, October 15, 2011. https://doi.org/10.1016/j.cej.2011.09.001 .
Publisher	Elsevier
Item record/more information	http://hdl.handle.net/10197/3976
Publisher's statement	This is the author's version of a work that was accepted for publication in Chemical Engineering Journal. Changes resulting from the publishing process, such as peer review, editing, corrections, structural formatting, and other quality control mechanisms may not be reflected in this document. Changes may have been made to this work since it was submitted for publication. A definitive version was subsequently published in Chemical Engineering Journal (Volume 174, Issue 1, 15 October 2011, Pages 206–212) DOI:# 10.1016/j.cej.2011.09.001 Elsevier Ltd.
Publisher's version (DOI)	10.1016/j.cej.2011.09.001

Downloaded 2026-05-01 23:47:22

The UCD community has made this article openly available. Please share how this access benefits you. Your story matters! (@ucd_oa)



© Some rights reserved. For more information

1 Transformation of beneficially reused aluminium sludge to potential P
2 and Al resource after employing as P-trapping material for wastewater
3 treatment in constructed wetland

4
5 X.H. Zhao*, Y.Q. Zhao and P. Kearney

6 *Centre for Water Resources Research, School of Civil, Structural & Environmental Engineering,*
7 *University College Dublin, Newstead, Belfield, Dublin 4, Ireland*

8
9 *Corresponding author. Tel.: +353-1-7163215; Fax: +353-1-7163297; E-mail: xiaohong.zhao@ucd.ie

10
11
12 **Abstract**

13 The phosphorus (P)-saturated aluminium sludge used as substrate in constructed wetland
14 (CW) for P-rich wastewater treatment was investigated to recover P and Al through chemical
15 precipitations of the P-extraction leachate of the used aluminium sludge. pH plays a key role
16 in such the precipitation processes. The obtained compounds were identified with XRD, FTIR
17 and SEM analyses. The results showed that over 99% PO_4^{3-} could be recovered as
18 hydroxyapatite by adding calcium chloride at pH of 13. The remaining Al could be fully
19 recovered as amorphous aluminium hydroxide at pH of 7.0 or alternatively as
20 Tris(8-hydroxyquinolino)aluminium (Alq_3) by adding suitable quantity of 8-hydroxyquinoline.
21 Although the purity, structure, characteristics and production control of the compounds are
22 worthy for further investigation, this study successfully developed a post-treatment
23 methodology for beneficially reused aluminium sludge. The significance of this study is not
24 only transferring aluminium sludge from “waste” to potential P and Al resources but also
25 reducing the environmental risk of final disposal of used aluminium sludge.

26 **Keywords:** P resource, aluminium sludge, P recovery, chemical precipitation

27 **1. Introduction**

28 Phosphorus (P) is essential to all living organisms since P is one of the vital components
29 of the DNA and the key element of the energy supplier ATP [1]. For human being, P is a
30 crucial contributor to human growth and metabolism, playing an important role in several
31 functions such as transformation of energy, synthesis of amino acids and proteins, generation
32 of vitamins and maintenance of bones and teeth etc. In modern society, there is a huge P
33 consumption in agriculture, industry and human food. Undoubtedly, agriculture is by far the
34 largest user of phosphate, accounting for 80-85% of total consumption. The consumption of
35 phosphate as fertilizers to improve the food production is also rising largely. Moreover, it has
36 been commonly recognized that the high quality reserves of P are being depleted
37 expeditiously and that the prevailing management of phosphate, a finite non-renewable source,
38 is not fully in accord with the principles of sustainability.

39 At the same time, the large amount of phosphate used worldwide leads to excess
40 quantities of P released into various water bodies via discharge of industrial effluent,
41 agriculture runoff, domestic wastewater etc., inducing eutrophication in surface waters and
42 resulting in a high environmental risk [2]. Therefore, regarding the sustainable development,
43 recovery P from wastewater has become a robust way in solving P pollution in waters and
44 relieving P resource crisis at the same time. In general, conventional P removal techniques in
45 wastewater treatment are based on the phosphate precipitation as iron or alum salt or fixation
46 in activated sludge through biological P removal. Unfortunately, huge amounts of the
47 resultant water-rich sludge including chemical sludge and/or activated sludge were generated
48 during these processes, leading to increasing costs for conditioning, dewatering and disposal
49 of these sludges. In addition, due to high water content and the low quality of the waste
50 sludges, reuse of P is not an economic attractive option. Thus, in recent year, some advanced
51 alternative techniques have been developed and applied to recover P from wastewater as
52 P-contained products which can be reused as resource. These include crystallization to obtain
53 struvite [3,4] or calcium phosphate [5,6] and ion exchange to achieve phosphoric acid [7,8]
54 etc.

55 High strength animal farm wastewater with P-rich characteristics has been studied
56 extensively at University College Dublin, Ireland, in incorporating dewatered alum sludge
57 cakes (DASC) as substrate into constructed wetlands (CW) to enhance the P removal. DASC
58 is an inevitable and easily available by-product derived from the drinking water purification
59 process with Al as main chemical component. The alum sludge-augmented constructed
60 wetland system has demonstrated an excellent ability of organics and nutrients especially P
61 removal/immobilization [9-11]. This pioneering development/investigation on the beneficial
62 reuse of DASC for P-rich wastewater treatment is now underway for eventual field
63 application [12].

64 However, recovery strategy of the immobilised P from the used/saturated DASC should
65 be studied to further promote the beneficial reuse of DASC in CW technology. Actually,
66 preliminary investigation has suggested a three-step procedure towards P recovery, which is:
67 1) P extraction from the used DASC, 2) decolouration of the P-extraction leachate and 3)
68 precipitation of phosphate compounds. The step 1) and 2) have been previously studied
69 [13,14]. Therefore, the objective of this study was to focus on the formation of phosphate
70 compounds and related issues from the decoloured P-extraction leachate of the used DASC in
71 CW system, thus transforming the used DASC to potential P resource.

72

73 **2. Materials and methods**

74 ***2.1 Decoloured P-extraction leachate***

75 Used/saturated DASC in CW system was firstly subjected to P-extraction using H₂SO₄
76 [13]. The resultant P-extraction leachate was actually a red-brown sulphuric acid leachate
77 (RSAL), which was then decoloured using a certain volume of H₂O₂ for oxidation. The
78 product of the decolorized sulphuric acid leachate (DSAL) was used for P precipitation step
79 [14]. The DSAL is a clear leachate with high concentrations of PO₄³⁻, Al and SO₄²⁻, as shown
80 in Table 1.

81

[Table 1]

82
83
84
85
86
87
88
89
90
91
92
93
94
95
96
97
98
99
100
101
102
103
104
105
106
107
108
109

It may be necessary to mention that the P-saturated DASC was obtained from a long-term operated laboratory scale CW system, which employed DASC as main substrate for a P-rich animal farm wastewater treatment trial with influent COD of 213 ± 127 mg/L; P of 28 ± 15 mg PO_4/L ; SS of 72 ± 66 mg/L and pH of 6.8 ± 0.4 . Originally, the DASC was collected directly from Ballymore-Eustace Water Treatment Plant in Southwest Dublin, Ireland, where aluminum sulphate was adopted as coagulant for reservoir water purification. After a long time of operation in the animal wastewater treatment system, the DASC (as substrate) was almost saturated with marginal P adsorption ability.

2.2 Precipitation methodology

2.2.1 Precipitation of calcium phosphate

Two series of 100 mL DSAL were adjusted by 10 M NaOH to pH range of 9-12 while $\text{CaCl}_2 \cdot 2\text{H}_2\text{O}$ (purchased from Riedel-deHaën Chemicals) was added with different molar ratio of Ca/P of 1.5 and 3, respectively. After reaction for 60 min, the precipitates were obtained and centrifuged at 3500 rpm for 15 min. The resultant precipitates were then washed by distilled water for at least three times before they were left for air-drying at room temperature for further characterization. The supernatant was analyzed for residual concentrations of P and Al. This allows optimising the reaction conditions for highest P precipitation efficiency.

Subsequently, two sets of 300 mL DSAL were used to conduct the precipitates tests to obtain the calcium phosphate at the particular pH of 13.0. In the first experimental set, calcium phosphates were formed in terms of CaP-1 while in the second experimental set, the large amount of sulphate ion (SO_4^{2-}) (in DSAL) was pre-immobilized by adding chemical equivalent quantity of $\text{BaCl}_2 \cdot 2\text{H}_2\text{O}$ (purchased from Riedel-deHaën Chemicals). The resultant precipitates of BaSO_4 were separated by centrifuging from the testing system. Thereafter, the remaining DSAL of set two experiment was subjected to calcium phosphate precipitation as the same as set one experiment by adding $\text{CaCl}_2 \cdot 2\text{H}_2\text{O}$. The precipitates were termed as CaP-2, which were then washed and air-dried for further characterization.

110 2.2.2 *Precipitation of aluminium compounds*

111 Although P was recovered by forming precipitate of calcium phosphate, great deal of
112 alum ion still remained in the DSAL. Subsequently, two methods were adopted to recover
113 Al^{3+} as aluminium compounds. The first process generated aluminium trihydroxide ($\text{Al}(\text{OH})_3$,
114 ATH) simply by adjusting pH to 7. The second process was to obtain
115 Tris(8-hydroxyquinolino)aluminium (Alq_3) via addition of suitable quantity of
116 8-hydroxyquinoline (purchased from AlfaAesar Chemicals). In Alq_3 precipitation, 100 mL
117 Al-rich solution/DSAL (in which P had been precipitated) was firstly adjusted by 10 M HCl
118 to a pH range of 6.0-6.5. Thereafter, 50 mL 8-Hydroxyquinoline-absolute ethanol solution,
119 which has a chemical equivalent quantity of 8-Hydroxyquinoline to aluminium, was added into
120 the Al-rich solution. After mixed sufficiently in a beaker, the beaker was then carefully put
121 into a water bath of 60-70 °C and stirred for 30 min. The yellow precipitates were therefore
122 observed, which can be separated by filtration. The resultant powder-like solids were washed
123 by alcohol and distilled water, and then air-dried for analysis.

124 Unless otherwise stated, all the experiments were carried out at room temperature and
125 replicated. The results were shown in average values. The entire precipitation experimental
126 procedure is schematically illustrated in Fig. 1.

127

128

[Figure 1]

129

130 2.3 *Analytical techniques*

131 The concentrations of P, Al, SO_4^{2-} and Colour in solution were analyzed using a Hach
132 spectrophotometer (DR/2800) according to the standard method. The pH was measured by pH
133 meter (ATI ORION, model 720A). The phase composition of the resultant compound powder
134 was determined on a X-ray diffraction (XRD) patterns using a Bruker D8 Advance
135 diffractometer (Germany) with Cu $\text{K}\alpha$ radiation ($\lambda = 1.5406$), operated at 40 kV and
136 40mA. The XRD data were collected over the 2θ range of 15-80° at

137 a scan speed of 1.5 min^{-1} with an increment of 0.01. The spectra of the precipitates were
138 measured by a Bruker Vector 70 Fourier-transform infrared spectrometer (FTIR) (Germany) to
139 indentify the nature of the bondings. The data was collected from the scan range of 4000-370
140 cm^{-1} . Samples were prepared by mixing powders of the composites with KBr. Pure KBr was
141 used as a background. The morphological structure and particle size of precipitates were
142 examined with Scanning Electron Microscope (SEM, JEOL JSM-T 300, Japan).

143

144 **3. Results**

145 ***3.1 Precipitation of calcium phosphate***

146 The results of initial P precipitation with $\text{CaCl}_2 \cdot 2\text{H}_2\text{O}$ at pH of 9-12 are shown in Fig. 2.
147 When the ratio of Ca/P is 1.5, over 98% P can be precipitated with calcium at the pH range
148 tested. The maximum P precipitation efficiency of 99.4% appeared at the pH of 9 and a light
149 decrease in efficiency was observed for higher pH values. However, it is interesting to see
150 that the P precipitation efficiency increased with increasing pH when the ratio of Ca/P is 3, at
151 which the maximum P precipitation of 99.9% can be obtained at pH 11. Comparing the cases
152 of different molar ratios of Ca/P, it is clear that the high ratio of Ca/P is favorable to achieve
153 the higher P precipitation efficiency. By inspecting the concentrations of residual Al,
154 obviously, almost all the Al could be precipitated simultaneously with P precipitation at the
155 pH of 9, but it reduced with increasing pH value. Interestingly, even at high pH of 12, 97.8%
156 of Al at Ca/P ratio of 1.5 and 94.5% of Al at Ca/P ratio of 3 could still be co-precipitated,
157 respectively, with the formation of calcium phosphate at the same time. Fig. 2 shows that the
158 pH range of 9 to 12 seemed not suitable to obtain the relatively pure calcium phosphate due to
159 the co-precipitation of Al. Thus, the subsequent experiments were carried out at higher pH
160 condition of 13 and the molar ratio of Ca/P was set up to 3.

161

162

[Figure 2]

163

164 The processes and results of the calcium phosphate formation at pH of 13 are illustrated in
165 Fig. 3. Here, Al^{3+} was well separated from PO_4^{3-} by adjusting pH to 13 with only 10% of Al^{3+}
166 mass loss (on average) being recorded. Two calcium phosphates in terms of CaP-1 and CaP-2,
167 respectively, were obtained. Clearly, SO_4^{2-} is also irrespective to the formation of calcium
168 phosphate and the main components of CaP-1 and CaP-2 should be the same which were
169 unveiled by XRD and FTIR analyses, as shown in Fig. 4a and Fig. 4b, respectively.

170

171 **[Figure 3]**

172 **[Figure 4]**

173

174 In XRD spectra, the characteristic peaks (at 2θ) appear at 26° and 32° which are almost
175 identical to those in stoichiometric microcrystalline hydroxyapatite ($\text{Ca}_{10}(\text{PO}_4)_6(\text{OH})_2$, HAP)
176 [15]. But the level of crystallization of powder is low due to the weak intensity of peaks. The
177 FTIR spectrum shows characteristic peaks at 560-610 and 1000-1100 cm^{-1} , being assigned to
178 PO_4^{3-} groups in the HAP resulting from P-O symmetric and asymmetric stretching and 3500
179 cm^{-1} correspond to the vibration of OH^- [16].

180 The microstructure of the powder CaP-2 was examined by SEM and is shown in Fig. 4c.
181 As it can be seen from the morphologies of the particles, there is a distribution of small
182 particles which show an approximately lamellar structure, and large agglomerates
183 consisting of fine particles. From visible photograph, the HAP obtained here is white powders,
184 as shown in Fig. 4d.

185

186 ***3.2 Precipitation of aluminium compounds***

187 In both the approaches of Al precipitation to form either $\text{Al}(\text{OH})_3$ (ATH) or Alq_3 , over
188 99% of the Al precipitation efficiency can be achieved, indicating that these two methods are
189 effective. XRD pattern and FTIR spectrum of the ATH powders are shown in Fig. 5a and b.
190 The diffuse peaks indicate that the product is amorphous. The characteristic peaks at 400-770
191 cm^{-1} belong to the vibration of Al-O group and those at 1068 and 1157 cm^{-1} imply the

192 stretching of O-H [17].

193

194 **[Figure 5]**

195

196 The SEM observation of ATH in Fig. 5c shows that the ATH samples consisted of small
197 particles and large agglomerates. From visible photograph shown in Fig. 5d, the ATH samples
198 look like white solid gel.

199 XRD pattern and FTIR of Alq₃ are shown in Fig. 6. From XRD, the main characteristic
200 peaks of Alq₃ at 2θ of 9.09, 10.34, 13.45, 15.53 and 24.16° were observed and the high level
201 crystallization appeared due to the high intensity of diffraction. Compared with other
202 compounds, the FTIR spectrum of Alq₃ is very complex but in accord with the reference [18].

203

204 **[Figure 6]**

205

206 From the observation of SEM (Fig. 6c) and visible photograph (Fig. 6d) of Alq₃, the Alq₃
207 is yellow needle-like solids and the SEM microphoto indicates that the microstructure of Alq₃
208 is cube pillar with diameter around 10 μm.

209

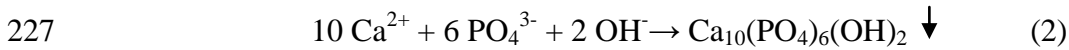
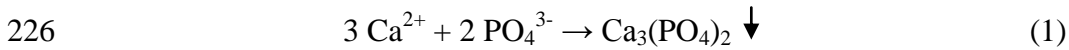
210 **4. Discussion**

211 ***4.1 P recovery process***

212 The main purpose of the current study was to explore an efficient and practically operated
213 methodology to recover P from DSAL. Since DSAL is a solution characterized with a great
214 deal of Al³⁺, PO₄³⁻, SO₄²⁻ and low pH value, the wet chemical method of precipitation should
215 be considered as the first choice. As is known, most of the phosphates are insoluble in
216 aqueous solution, such as aluminium, ferric and calcium phosphates. Therefore, considering
217 the fact that there still has large amount of Al³⁺ in DSAL, the attempt of forming AlPO₄
218 precipitation has been carried out firstly and reported elsewhere [19]. Although P can be
219 recovered as AlPO₄ from solution only through pH adjustment by adding alkali, through

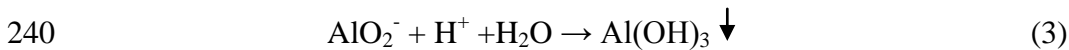
220 inspecting the mass balance, it should be pointed out that the resultant precipitation is a
221 mixture mainly consisted of amorphous AlPO_4 and Al(OH)_3 due to the surplus Al in the
222 system [19]. The excess Al should be co-precipitated with AlPO_4 by forming Al(OH)_3 at the
223 pH of 6. For this reason, precipitation of calcium phosphates was considered.

224 PO_4^{3-} can be precipitated by Ca^{2+} under alkaline condition to form calcium phosphates
225 which could be expressed in Eq. (1) and (2).



228 Low pH benefits precipitation of $\text{Ca}_3(\text{PO}_4)_2$, whereas the formation of hydroxyapatite is
229 dominant as long as the pH value is higher than 10 [20]. In current study, however, if pH
230 value is adjusted to 9-12, most of Al^{3+} can be precipitated as Al(OH)_3 , leading to a negative
231 effect on the purity of hydroxyapatite. Therefore, a further increase of pH up to 13 was
232 proposed, in which Al(OH)_3 can be dissolved to AlO_2^- . As a result, considerably pure
233 hydroxyapatite was obtained which has been identified by XRD and FTIR analyses (see Fig. 4).
234 Accordingly, the Ca/P ration is 1.67. Normally, calcium phosphates were widely used as a
235 long-term fertilizer. Bioactive calcium phosphate ceramics such as hydroxyapatite and
236 tricalcium phosphate have been widely used as bone graft materials. That is the reason of
237 more attentions having been paid to their syntheses, characterization and application [21,22].

238 After immobilizing PO_4^{3-} under pH 13, aluminium can be precipitated as Al(OH)_3 by
239 adjusting the pH to 7 according to the reaction showing in Eq. (3).

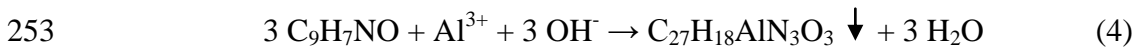


241 It can be seen from the XRD pattern (see Fig. 5) that, even though most of the Al(OH)_3
242 are amorphous, a small portion the bayerite ($\alpha\text{-Al(OH)}_3$) phase can still be recognized by their
243 major diffraction peaks at $2\theta = 20.14^\circ$ and 40.34° , respectively, although they are weak and
244 broad. This result is accordant with other study reported from the literature [23].

245 Al(OH)_3 is a common source for producing aluminum oxides which have wide
246 applications in catalysts, ceramics, capacitors, and substrates for integrate circuits etc. The

247 resultant powder from this study may be potentially used as a raw industrial material.

248 Alternatively, Alq₃ can be formed in the DSAL solution after PO₄³⁻ is immobilized. Alq₃ is
249 an organic electronic material and could be used as an efficient electroluminescent material
250 [24] for OLED use in the next generation of display [25,26]. It can be produced by the
251 reaction of Al³⁺ and 8-hydroxyquinoline (C₉H₇NO) (see Eq. (4)) under the pH range of
252 4.2-9.8 [18].



254 The spatial framework and the molecular structure of Alq₃ are illustrated in Fig. 7 [27].
255 Obviously, the structure is such that the central Al atom is surrounded by the three quinolate
256 ligands in a pseudooctahedral configuration with the A- and C-quinolate nitrogens and the B-
257 and C-quinolate oxygen trans to each other. Because of complication of its structure, large
258 numbers of sharp absorption peaks appeared in FTIR spectra which are contributed with
259 vibration C=C, C-N, C-O, C-H, Al-O, -OH and the ring of quinoline etc. (see Fig. 6).

260

261 **[Figure 7]**

262

263 The results shown in Fig. 3 indicated that the SO₄²⁻ has no negative effect on the formation
264 of calcium phosphates. Therefore, considering the economic issue and the simplification of
265 operation, there is no requirement to remove SO₄²⁻ first. Overall, through easy-handling
266 chemical reactions, the main components, P and Al, of used DASC in CW system could be
267 recovered successfully as different compounds such as aluminum phosphate, hydroxyapatite,
268 aluminum hydroxide, and Alq₃.

269 ***4.2 Significance of this study***

270 Regarding P elimination in constructed wetland system, the performance mainly depends
271 on the adsorption ability of substrate. Since the generally employed substrates, i.e. gravel,
272 sand or soil, have low capacity for P trapping, prominent research goals of CW has being
273 focused on seeking specialized substrates with conductive physicochemical characteristics to

274 improved P removal. A great variety of different novel types of materials, including natural
275 products such as Laterite [28] and peat [29], industrial by-products like slag [30], coal fly
276 ashes [31] and man-made products like LECA [32] and Filtra P [33], have been reported in
277 literatures.

278 As an inevitable and huge output by-product of drinking water treatment plants, the
279 expense for disposing DASC to landfill site increases gradually. Therefore, employment of
280 DASC as main substrate for P trapping has a remarkable significance of transferring a
281 “waste” to raw material which could be combined with CW to enhance the capacity of P
282 retention, making alum sludge-based CW system served like a P sink. The results obtained
283 from the current study demonstrated that a large amount of P in used/saturated DASC could
284 be recovered as P compounds through some chemical processes, developing a suitable and
285 effective methods for used DASC post-treatment in which not only P compounds could be
286 achieved but also the environment risk for used DASC final disposal could be reduced as well.
287 Additionally, without a doubt, the usefulness of recovered P compounds can be justified as
288 raw materials used in many areas.

289 It should be noted that commercial phosphates are mainly produced from natural
290 phosphate rock. Even though the price of the natural phosphate rock has an increasing tend,
291 for example the price of phosphate rock from Morocco remained below 50 US \$/ton up to
292 2006 and went up to more than 300 US \$/ton by 2008 with peaks around 1,000 US \$/ton [34].
293 The recovered P is even more expensive. Balmé [35] calculated the costs of about 3,600
294 euro/ton P for a P recovery from wastewater in combination with P elimination. For P
295 recovery from sewage sludge, the costs could be about 8,800 euro/ton P. From the calculation
296 based on this laboratory scale P recovery study, the chemical investment can be 0.68 euro/g P.
297 However, for practical use the chemical cost could be low. Nevertheless, it should be noted
298 that the P recovery is an expensive process.

299 Although the purity, structure, characteristics and production control of the compounds
300 are worthy for further investigation, this work successfully explored the methodology to
301 transformation of the used DSAC in CW system as potential resource for P recovery after

302 employment of DASC as P trapping material for wastewater treatment.

303

304 **5. Conclusions**

305 Chemical precipitation was adopted to separate Al^{3+} , PO_4^{3-} and SO_4^{2-} from DSAL. pH is
306 the key factor for such the precipitation process. When pH of the DSAL is adjusted to 13, Al^{3+}
307 turns to AlO_2^- and $\text{Al}(\text{OH})_3$ cannot be formed. Therefore, over 99% PO_4^{3-} could be recovered
308 as hydroxyapatite by adding calcium chloride. Thereafter, aluminium remained in the solution
309 could be precipitated as $\text{Al}(\text{OH})_3$ gel after adjusting the pH to 7. Alternatively, aluminium
310 remained in the solution could be precipitated as Alq_3 by adding suitable quantity of
311 8-hydroxyquinoline. Although SO_4^{2-} has no adverse effect on the precipitation process of
312 either aluminium phosphate or hydroxyapatite, it could be immobilized by barium salt. To
313 characterize all the precipitations obtained, XRD and FTIR analyses and SEM and visible
314 photograph were employed to assist the identification of the various precipitations. Overall,
315 this study explored and developed an effective and consistent methodology to recover P and
316 Al as potential P and Al resources from DASC after employment as substrate in CWs for
317 wastewater treatment.

318

319 **Acknowledgements**

320 The authors would like to acknowledge the research funding provided by the
321 Environmental Protection Agency, Ireland through the Environmental Technologies Scheme
322 (project no. 2005-ET-MS-38-M3). The first author wishes to thank University College Dublin
323 for the *Ad Astra* scholarship. In particular, the authors appreciate the technical assistance
324 provided by Guangzhou Institute of Geochemistry and Jinan University, Guangzhou, P.R.
325 China during this study.

326

327 **References**

- 328 [1] P. Steen, Phosphorus availability in the 21st century, *Phosphorus and Potassium* 217(Sep.-Oct.)
329 (1998) 25-31.
- 330 [2] S. Burke, L. Heathwaite, N. Preedy, Transfer of phosphorus to surface waters: Eutrophication, In
331 Valsami-Jones, E. (ed.), *Phosphorus in environmental technologies: Principles and application*.
332 London: IWA publishing (2004) pp.120-146.
- 333 [3] J.D. Doyle, K. Oldring, J. Churchley, C. Price, S.A. Parsons, Chemical control of struvite
334 precipitation, *J. Environ. Eng.-ASCE* 129 (2003) 419-426.
- 335 [4] K.S. Le Corre, E. Valsami-Jones, P. Hobbs, S.A. Parsons, Phosphorus recovery from wastewater
336 by struvite crystallization: a review, *Crit. Rev. Env. Sci. Tec.* 39 (2009) 433-477.
- 337 [5] U. Berg, D. Donnert, P.G. Weidler, E. Kaschka, G. Knoll, R. Nüesch, Phosphorus removal and
338 recovery from wastewater by tobermorite-seeded crystallisation of calcium phosphate, *Water Sci.*
339 *Technol.* 53 (2006) 131-138.
- 340 [6] Y. Song, P.G. Weidler, U. Berg, R. Nüesch, D. Donnert, Calcite-seeded crystallization of calcium
341 phosphate for phosphorus recovery, *Chemosphere* 63 (2006) 236-243.
- 342 [7] N.I. Chubar, V.A. Kanibolotsky, V.V. Strelko, G.G. Gallios, V.F. Samanidou, T.O.
343 Shaposhnikova, V.G. Milgrandt, I.Z. Zhuravlev, Adsorption of phosphate ions on novel inorganic
344 ion exchangers, *Colloid Surface A* 255 (2005) 55-63.
- 345 [8] I. Midorikawa, H. Aoki, A. Omori, T. Shimizu, Y. Kawaguchi, K. Kassai, T. Murakami, Recovery
346 of high purity phosphorus from municipal wastewater secondary effluent by a high-speed
347 adsorbent, *Water Sci. Technol.* 58 (2008) 1601-1607.
- 348 [9] Y.Q. Zhao, A.O. Babatunde, X.H. Zhao, W.C. Li, Development of alum sludge-based constructed
349 wetland: An innovative and cost effective system for wastewater treatment, *J. Environ. Sci. Heal.*
350 *A* 44 (2009) 827-832.
- 351 [10] A.O. Babatunde, Y.Q. Zhao, A.M. Burke, M.A. Morris, J.P. Hanrahan, Characterization of
352 aluminium-based water treatment residual for potential phosphorus removal in engineered
353 wetlands, *Environ. Pollut.* 157 (2009) 2830-2836.
- 354 [11] A.O. Babatunde, Y.Q. Zhao, X.H. Zhao, Alum sludge-based constructed wetland system for
355 enhance removal of P and OM from wastewater: Concept, design and performance analysis,

- 356 Bioresource Technol. 101 (2010) 6576-6579.
- 357 [12] Y.Q. Zhao, A.O. Babatunde, Y.S. Hu, J.L.G. Kumar, X.H. Zhao, Pilot field-scale demonstration
358 of a novel alum sludge-based constructed wetland system for enhanced wastewater treatment,
359 Process Biochem 46 (2011) 278-283.
- 360 [13] X.H. Zhao, Y.Q. Zhao, Investigation of phosphorus desorption from P-saturated alum sludge used
361 as a substrate in constructed wetland, Sep. Purif. Technol. 66 (2009a) 71-75.
- 362 [14] X.H. Zhao, Y.Q. Zhao, Decolouration of H₂SO₄ leachate from phosphorus-saturated alum sludge
363 using H₂O₂ and advanced oxidation processes in phosphorus recovery strategy, J. Environ. Sci.
364 Heal. A 44 (2009b) 1557-1564.
- 365 [15] S. Cai, X. Yu, Z. Xiao, G. Xu, H. Lv, K. Yao, Synthesis and sintering of nanocrystalline
366 hydroxyapatite powders by gelatine-based precipitation method, Ceram. Int. 33 (2007) 193-196.
- 367 [16] I. Mobasherpour, M. Soulati Heshajin, A. Kazemzadeh, M. Zakeri, Synthesis of nanocrystalline
368 hydroxyapatite by using precipitation method, J. Alloy. Compd. 430 (2007) 330-333.
- 369 [17] S. Music, D. Dragcevic, S. Popovic, Hydrothermal crystallization of boehmite from freshly
370 precipitated aluminium hydroxide, Mater. Lett. 40 (1999) 269-274.
- 371 [18] H. Li, F. Zhang, D. Zheng, Investigation on structural characteristics of tri-(8-hydroxyquinoline)
372 aluminium, Chinese Journal of Luminescence 24 (2003) 44-50.
- 373 [19] X.H. Zhao, Y.Q. Zhao, P. Kearney, Recovery of AlPO₄ from beneficially reused
374 Aluminium-water treatment sludge, Water Sci. Technol. (under review).
- 375 [20] C. Liu, Y. Huang, W. Shen, J. Cui, Kinetics of hydroxyapatite precipitation at pH 10 to 11,
376 Biomaterials 22 (2001) 301-306.
- 377 [21] J. Liu, X. Ye, H. Wang, M. Zhu, B. Wang, H. Yan, The influence of pH and temperature on the
378 morphology of hydroxyapatite synthesized by hydrothermal method, Ceram. Int. 29 (2003)
379 629-633.
- 380 [22] G. Sun, Y.Q. Zhao, S.J. Allen, An alternative arrangement of gravel media in tidal flow reed beds
381 treating pig farm wastewater, Water Air Soil Pollut. 182 (2007) 13-19.
- 382 [23] X. Du, Y. Wang, X. Su, J. Li, Influences of pH value on the microstructure and phase
383 transformation of aluminium hydroxide, Powder Technol. 192 (2009) 40-46.

- 384 [24] C.W. Tang, S.A. VanSlyke, Organic electroluminescent diodes, *Appl. Phys. Lett.* 51 (1987)
385 913-915.
- 386 [25] G. Sun, Y.Q. Zhao, S.J. Allen, D. Cooper, Generating “Tide” in pilot-scale constructed wetlands
387 to enhance agricultural wastewater treatment, *Engineering in Life Sciences* 6 (2006) 560-565.
- 388 [26] E.L. Williams, K. Haavisto, J. Li, G.E. Jabbour, Excimer-Based White Phosphorescent Organic
389 Light-Emitting Diodes with Nearly 100% Internal Quantum Efficiency, *Adv. Mater.* 19 (2007)
390 197-202.
- 391 [27] A. Irfan, R. Cui, J. Zhang, Energy decomposition analysis of methyl derivatives of the meridional
392 isomer of tris(8-hydroxyquinolino)aluminium (mer-Alq₃), *Chem. Phys.* 358 (2009) 25-29.
- 393 [28] R.B. Wood, C.F. McAtamney, Constructed wetlands for waste water treatment: the use of laterite
394 in the bed medium in phosphorus and heavy metal removal, *Hydrobiologia* 340 (1996) 323-331.
- 395 [29] P.A. Brown, S.A. Gill, S.J. Allen, Metal removal from wastewater using peat, *Water Res.* 34
396 (2000) 3907-3916.
- 397 [30] C. Vohla, M. Kõva, H.J. Bavor, F. Chazarenc, ü Mander, Filter materials for phosphorus removal
398 from wastewater in treatment Wetlands-A review, *Ecol. Eng.* 37 (2011) 70-89.
- 399 [31] J. Chen, H. Kong, D. Wu, Z. Hu, Z. Wang, Y. Wang, Removal of phosphate from aqueous
400 solution by zeolite synthesized from fly ash, *J. Colloid Interf. Sci.* 300 (2006) 491-497.
- 401 [32] M.E. Kvarnstrom, C.A.L. Morel, T. Krogstad, Plant-availability of phosphorus in filter substrates
402 derived from small-scale wastewater treatment systems, *Ecol. Eng.* 22 (2004) 1-15.
- 403 [33] J.P. Gustafsson, A. Renman, G. Renman, K. Poll, Phosphate removal by mineral-based sorbents
404 used in filters for small-scale wastewater treatment, *Water Res.* 42 (2008) 189-197.
- 405 [34] A. Pickett, The outlook for STPP, *Phosphates 2008 International Conference and Exhibition*,
406 Paris, 17-19 Feb. 2008.
- 407 [35] P. Balmér, Phosphorus recovery, an overview of potential and possibilities. *IWA Specialist*
408 *Conference. Wastewater Sludge as a Resource*, Trondheim, Norway, 23-25 June. 2003.

409

410

411

412

413 **Figure Caption**

414 **Fig. 1** Schematic illustration of P recovery processes

415 **Fig. 2** Effect of pH and the ratio of Ca/P on the precipitation process of calcium phosphate

416 **Fig. 3** Calcium phosphate formation with and without SO_4^{2-}

417 **Fig. 4** XRD pattern (a), FTIR spectra (b), SEM (c) and visible photograph (d) of resultant calcium
418 phosphate

419 **Fig. 5** XRD pattern (a), FTIR spectra (b), SEM (c) and visible photograph (d) of aluminium
420 hydroxide (ATH)

421 **Fig. 6** XRD pattern (a), FTIR spectra (b), SEM (c) and visible photograph (d) of Alq_3

422 **Fig. 7** The geometry of mer- Alq_3 with labels A–C for three quinolate ligands (a) and
423 The molecular structure of Alq_3 (b)

424

425

426

427

428

429

430

431

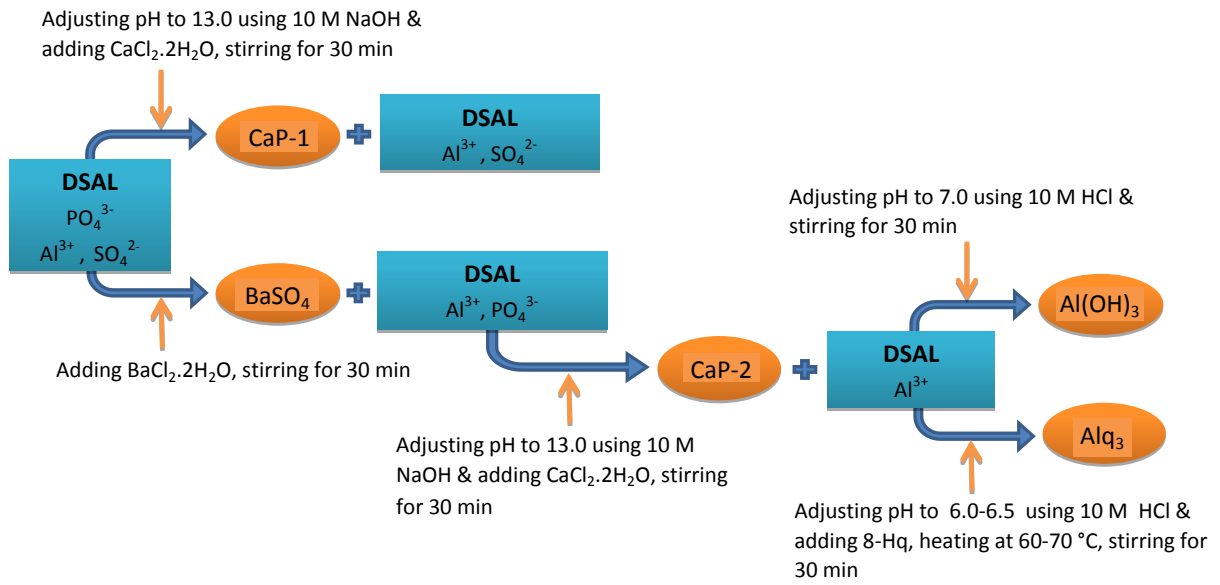
432

433

434

435

436



438

439

Fig. 1 Schematic illustration of P recovery processes

440

441

442

443

444

445

446

447

448

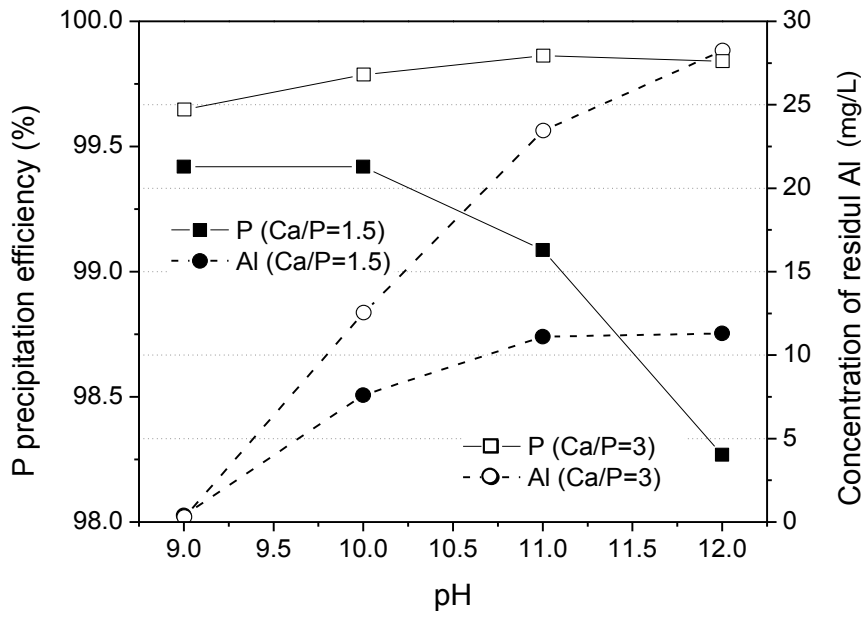
449

450

451

452

453



455

456

Fig. 2 Effect of pH and the ratio of Ca/P on the precipitation process of calcium phosphate

457

458

459

460

461

462

463

464

465

466

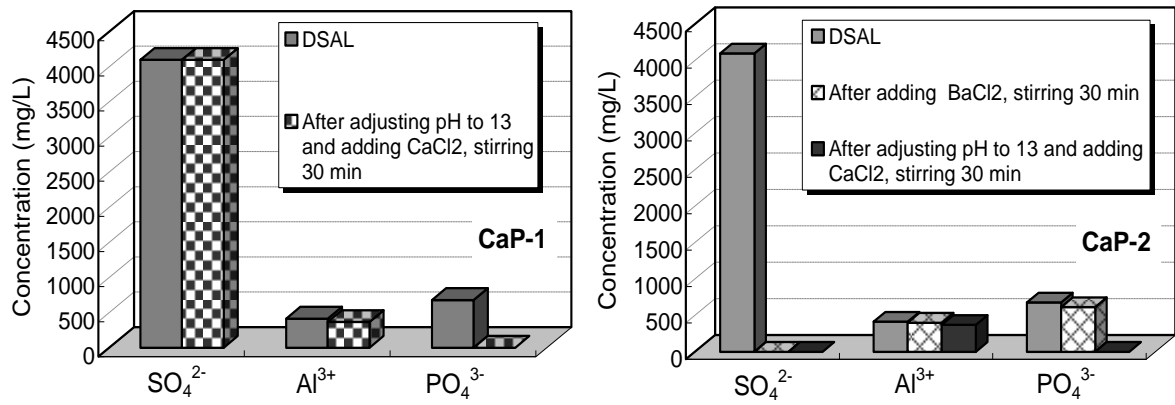
467

468

469

470

471



472

473

Fig. 3 Calcium phosphate formation with and without SO_4^{2-}

474

475

476

477

478

479

480

481

482

483

484

485

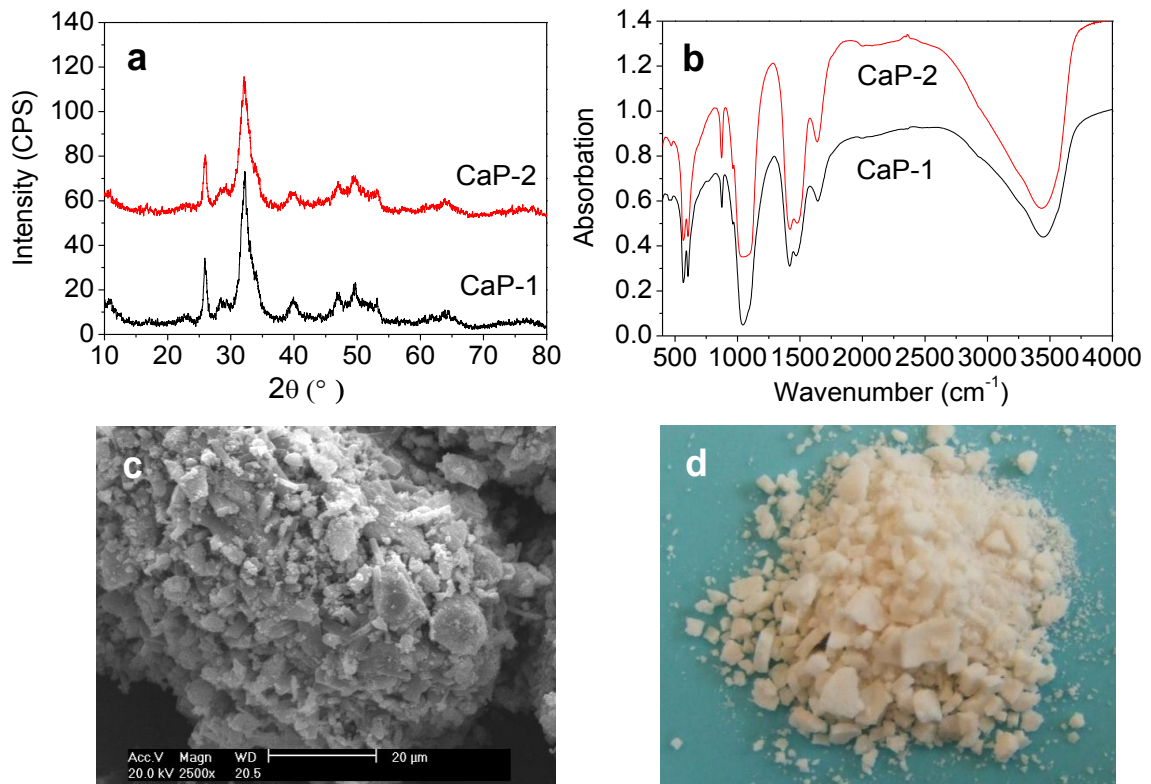
486

487

488

489

490



492

493

Fig. 4 XRD pattern (a), FTIR spectra (b), SEM (c) and visible photograph (d) of resultant calcium phosphate

494

495

496

497

498

499

500

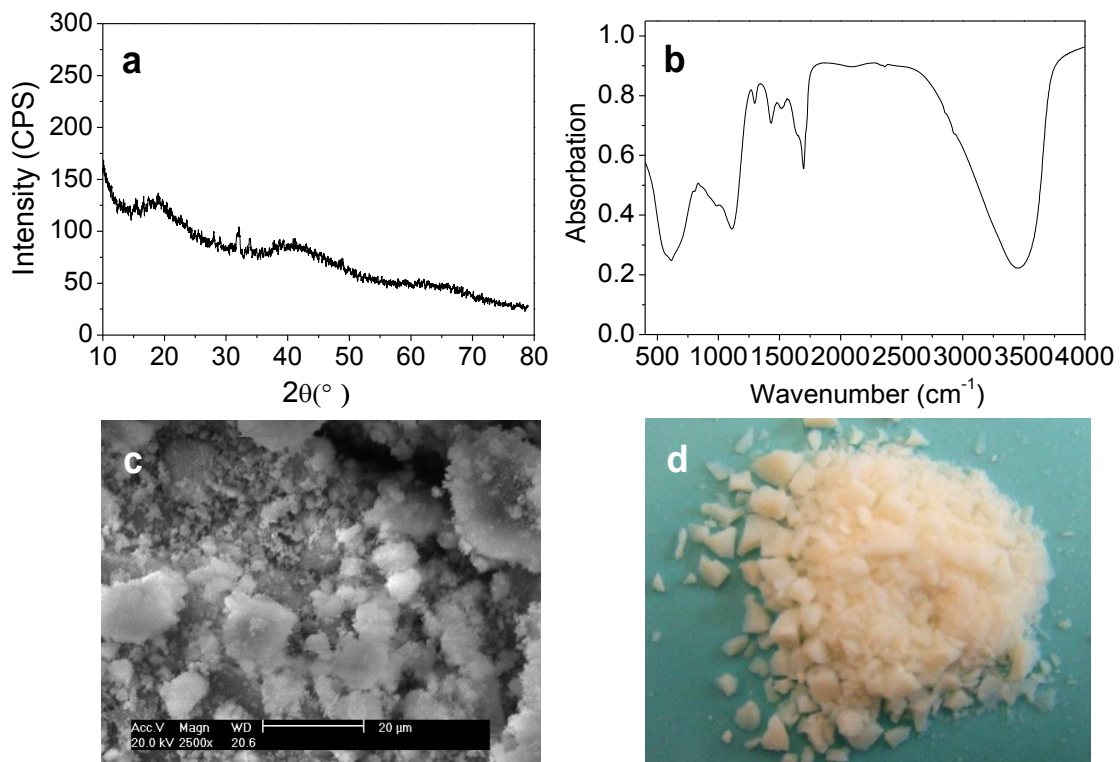
501

502

503

504

505



506

507 **Fig. 5** XRD pattern (a), FTIR spectra (b), SEM (c) and visible photograph (d) of aluminium
508 hydroxide (ATH)

509

510

511

512

513

514

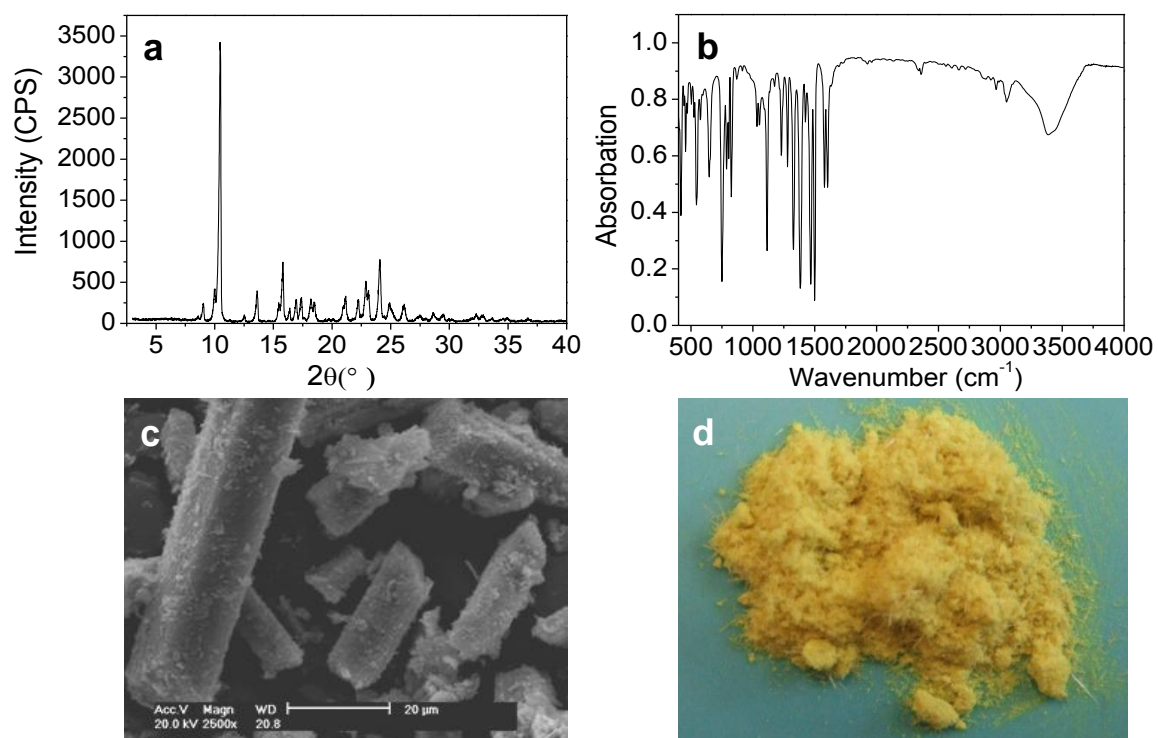
515

516

517

518

519



521

522

Fig. 6 XRD pattern (a), FTIR spectra (b), SEM (c) and visible photograph (d) of Alq₃

523

524

525

526

527

528

529

530

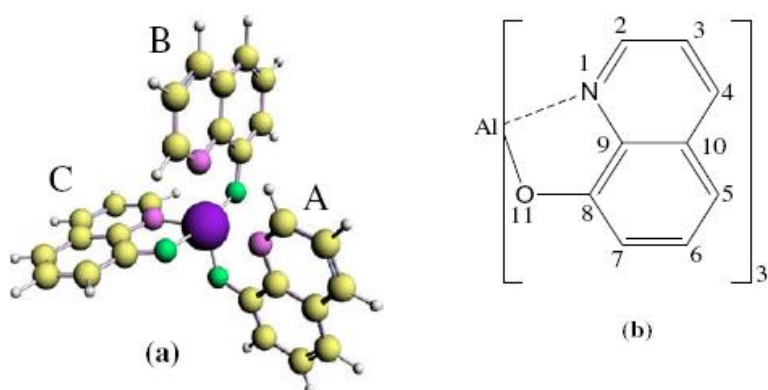
531

532

533

534

535



536

537 **Fig. 7** The geometry of mer-Alq₃ with labels A–C for three quinolate ligands (a) and
538 The molecular structure of Alq₃ (b) [27]

539

540

541

542

543

544

545

546

547

548

549

550

551

552

553

554

555 **Table Caption**

556 **Table 1** The characteristics of DSAL

557

558

Table 1 The characteristics of DSAL

	pH	Colour (Pt-Co units)	TOC (mg/L)	P (as PO ₄ ³⁻) (mg/L)	Al (mg/L)	SO ₄ ²⁻ (mg/L)
DSAL	~1.9	0	94	680	414	4100

559